Simultaneous Removal of Methyl Orange and Cr(VI) Using Polyethyleneimine-modified Corncob-derived Carbon Material

Yang Liu, Song Wang,* Yong Liang, Huan Zhou, Xinshu Li, Lin Duan, Shuang Chen, Sanxi Li, Linnan Zhang, and Ailing Zhang

Polyethyleneimine (PEI) modified corncob-derived carbon material (CCM) was prepared by the simple wet-impregnation technique. Field emission scanning electron microscopy (FESEM), energy-dispersive X-ray spectroscopy (EDS), Fourier-transform infrared spectroscopy (FT-IR), and nitrogen isothermal adsorption/desorption measurements were used to compare the structural differences between the CCM and the PEI-modified CCM (PEI-CCM). In the single-pollutant removal experiment, the PEI-CCM showed high adsorption capacities for methyl orange (MO) and Cr(VI). However, the CCM only showed high adsorption capacity for MO. Moreover, the PEI-CCM exhibited high removal efficiencies in the simultaneous removal of MO and Cr(VI), with final removal efficiencies of 100% and 95%, respectively. The reusability experiment of PEI-CCM indicated that, after four recycles, PEI-CCM maintained high performance with the removal efficiency of MO and Cr(VI) decreased less than 3% and 16%, respectively. The prepared PEI-CCM could be a high-performance adsorbent for the simultaneous removal of MO and Cr(VI) from water containing multiple pollutants.

Keywords: Polyethyleneimine; Methyl orange; Cr(VI); Adsorption; Corncob; Waste management; Biochar

Contact information: School of Environmental and Chemical Engineering, Shenyang University of Technology, Shenyang 110870, China;
** Corresponding author: wangsong@sut.edu.cn*

INTRODUCTION

With increasing concern for environmental protection, more attention is being paid to the harmful effects of water pollution, and heavy metals compose a considerable proportion of water pollution (Pan and Zhao 2019). Most heavy metal ions, such as Cr(VI), Cu(II), Cd(II), and Pb(II), are highly toxic and easily accumulate in the biological chain, which can be harmful to human health and the environment (Norouzi *et al*. 2018; de Freitas *et al*. 2019). Dye pollution is another serious type of water pollution (Amin *et al*. 2019). The discharge of dye wastewater can reduce the transparency of the water body and consume the oxygen in the water, which can affect the survival of aquatic species and destroy the water body's self-purification ability (Gao *et al*. 2017). Moreover, due to potential mutagenic dyes such as methyl orange (MO) and methylene blue (MB), exposure to dye wastewater can increase the risk of tachycardia, jaundice, and quadriplegia. In some textile and manufacturing industries, the simultaneous application of heavy metal ions and dyes causes a complex composition of the wastewater (Liu *et al*. 2018; Mishra and Maiti 2019). Therefore, the ability to simultaneously remove heavy metal ions and dyes is becoming increasingly important.

Many methods have been developed to remove these pollutants, including chemical precipitation, membrane separation, solvent extraction, and physical adsorption. Some of these techniques have notable shortcomings, including low removal efficiency, high removal cost, and long removal time. Compared with other techniques, adsorption has the advantages of easy operation, high efficiency, and low cost. Because the properties of the adsorbent greatly affect its performance, many efficient adsorbents have been developed in recent years. These include layered double hydroxides (Zheng *et al.* 2019), metal-organic frameworks, carbon materials (Zhang *et al*. 2019), and porous silicas (Liu *et al.* 2019a). However, adsorbents have some disadvantages, such as complex preparation procedures and unsatisfactory treatment of the contaminated adsorbent which had been used and should be disposed.

Due to the low feedstock cost, the use of waste materials to prepare high-performance materials has drawn increasing attention (Song *et al.* 2019). Agricultural waste is a type of renewable and low-cost biomass resource (Wang *et al*. 2020a). Using agricultural waste to prepare carbon materials is an efficient way to obtain high-performance adsorbent (Li *et al.* 2019). Various agricultural wastes such as coffee grounds (Wang *et al*. 2019; Wen *et al*. 2019), coconut waste (Rahim *et al.* 2019), and *Citrus reticulata* shells (Santos *et al*. 2015) have been used as feedstocks to prepare adsorbents. These agricultural-waste-derived adsorbents have been successfully used in the treatment of heavy metal wastewater or dye wastewater and exhibited high removal efficiency (Rathinam *et al*. 2018). However, the simultaneous removal of multiple pollutants is still a challenge for them (Chen *et al*. 2018a). To enhance the removal efficiency and expand the application field of these agricultural-waste-derived adsorbents, a chemical modification technique has been developed. Using this technique, the surface functional groups of the adsorbent can be adjusted, and the adsorption ability of the adsorbent can be improved (Sun *et al*. 2016). Polyethyleneimine (PEI) is an attractive chemical modification agent because its molecules contain many amine groups, which can strongly interact with negatively charged hydrophilic pollutants (Lv *et al*. 2018). However, a cross-linking agent such as glutaraldehyde is sometimes needed in the PEI modification process (Ma *et al.* 2014).

Corncob is an important agricultural waste, with approximately 28 million tons generated globally each year (Laleicke 2018; Li *et al*. 2018a). Using corncob as a feedstock to prepare adsorbent can both affect resource recycling and also benefit the environment. Thus, a wet-impregnation method, which does not need a cross-linking agent, was conducted to modify corncob-derived carbon material (CCM) with PEI. The as-prepared PEI-modified CCM (PEI-CCM) was applied in the removal of MO and Cr(VI). The structure of the PEI-CCM was characterized, and its adsorption mechanism was investigated using isothermal adsorption and kinetic models. Simultaneous removal of MO and Cr(VI) by the PEI-CCM was also evaluated.

EXPERIMENTAL

Materials

Corncob waste was collected from a local field in Fushun County, Liaoning, China. The PEI (molecular weight of 3,000 g/mol) was obtained from Shanghai Gobekie New Material Technology Co., Ltd. (Shanghai, China). Phosphoric acid (H_3PO_4, 85%) was purchased from Sinopharm Chemical Reagent Co., Ltd. (Shanghai, China). Other chemical reagents, including potassium dichromate and methanol, were purchased from Tianjin

Damao Chemical Reagent Factory (Tianjin, China). All these obtained analytical grade reagents were used directly without further purification.

Preparation of PEI-CCM adsorbent

First, corncob waste was ground into particles and passed through a 100-mesh (149-μm) nylon sieve. Then, the sifted corncob waste particles were washed five times with distilled water to remove surface-attached dust. The cleaned corncob waste particles were dried in an oven at 120 °C for 24 h. The dried corncob waste particles were blended with H_3PO_4 at a ratio of 0.34 mol H_3PO_4 / 10 g of corncob waste particles), after which 60 mL of distilled water was added. Then, the mixture was blended at 80 °C for 2 h. After that, the mixture was heated to 130 °C to evaporate water. The obtained residue was heated in a furnace to 500 °C for 2 h under nitrogen atmosphere. The as-prepared sample was washed with distilled water until neutral. After drying at 100 °C for 24 h, the CCM was obtained.

Based on the fact that PEI can be easily grafted on the surface of carbon material through amidation reaction, the modification of the CCM by the PEI was performed by the wet-impregnation method (Geng *et al*. 2019). The CCM (1 g) and PEI (0.4 g) were added to 20 mL of methanol and stirred at 30 °C for 12 h. After the evaporation of the methanol at 80 °C for 2 h, the obtained particles were washed with 50 mL of methanol three times to remove the residual PEI, which is soluble in methanol and can be washed off by this process as reported in literature (Quan *et al*. 2019). After filtration, the obtained carbon material was heat-treated at 80 °C for 6 h in an oven, and the final product was denoted as PEI-CCM.

Characterization

The surface morphologies and chemical compositions of the samples were examined with a field emission scanning electron microscope (Hitachi SU8010N, Tokyo, Japan) equipped with an energy-dispersive X-ray spectrometer. The functional groups of the samples were measured with a Fourier-transform infrared spectrophotometer (Shimadzu Prestige-21, Kyoto, Japan) using the KBr tablet method. The specific surface areas and pore size distributions of the samples were determined using an ASAP 2460 analyzer (Micrometrics, Norcross, GA, USA).

Adsorption experiments

The adsorption experiments of MO and Cr(VI) were performed in a mechanical shaker (Chen *et al*. 2019a). The pH value of the adsorption solution was adjusted with a 0.1 M HCl solution. To study the MO removal ability of the PEI-CCM, the adsorption temperature was set at 35 °C, and the pH value of the MO solution was set at 7. Ten milligrams of the PEI-CCM was added to 50 mL of MO solution to start the adsorption process. After the adsorption process, the suspension was filtered using a syringe filter with a pore size of 0.22 μm. The concentration of MO in the filtrate was measured using a T6 UV–Vis spectrophotometer (Beijing Purkinje General Instrument Co., Ltd., Beijing, China) at a wavelength of 464 nm (Lu *et al*. 2016). The Cr(VI) adsorption experiments were conducted at a temperature of 35 °C and solution pH of 5.7. Twenty-five milligrams of the PEI-CCM was added to 50 mL of Cr(VI) solution. The suspension was filtered by a syringe filter with a pore size of 0.22 μm after adsorption. Then, the obtained filtrate was treated with 1,5-diphenylcarbazide. The concentration of Cr(VI) in the filtrate was measured by the UV–Vis spectrophotometer at a wavelength of 540 nm (Wang *et al*. 2020b).

The adsorption capacity of the PEI-CCM (Q_e, mg/g) and removal efficiency of the adsorbate (R_e, %) were calculated according to Eqs. 1 and 2,

$$Q_e = \frac{(C_0 - C_e) \times V}{m} \quad (1)$$

$$R_e = \left(\frac{C_0 - C_e}{C_0}\right) \times 100\% \quad (2)$$

where C_0 (mg/L) is the initial concentration of the adsorbate, C_e (mg/L) is the equilibrium concentration of the adsorbate, V (L) is the solution volume, and m (g) is the adsorbent weight, as reported in the literature (Chen *et al*. 2020; Zhang *et al*. 2020).

Experiments for the simultaneous removal of MO and Cr(VI) by the PEI-CCM were conducted at 35 °C, and the pH value of the binary adsorbate solution was set at 5.7. The concentrations of MO and Cr(VI) were both set at 20 mg/L. During the equilibrium adsorption isotherm experiment, 25 mg of adsorbent was added to the 50-mL binary adsorbate solution.

Regeneration of the Used PEI-CCM

To examine the reusability of the PEI-CCM adsorbent, an adsorption-desorption experiment was performed. The used PEI-CCM adsorbent was stirred in 1 M NaOH solution for 1 h to release the adsorbed chromium ions (Lv *et al*. 2018). Then, the treated PEI-CCM adsorbent was washed using methanol to remove the MO. After drying at 100 °C for 2 h, the PEI-CCM adsorbent was added to the binary adsorbate solution to start the next experiment. The regenerated PEI-CCM was reused as the adsorbent four times. The reusability experiment of PEI-CCM was conducted at 35 °C. The pH value of the binary adsorbate solution was set at 5.7. The concentrations of MO and Cr(VI) were both set at 20 mg/L. The adsorption time was 400 minutes.

RESULTS AND DISCUSSION

Characterizations of Adsorbents

Table 1 and Fig. 1 present energy-dispersive X-ray spectroscopy (EDS) and the field emission scanning electron microscopy (FESEM) investigation results for the CCM and the PEI-CCM. The CCM and PEI-CCM exhibited similar surface morphologies. Coral-like structures formed by the irregular aggregation of holes and particles were observed on the particle surface. The elemental compositions of the CCM and PEI-CCM were different. The CCM was 92.5% C and 7.5% O, while the PEI-CCM was 81.0% C, 12.1% O, and 6.85% N. Polyethyleneimine contains a certain amount of amines, so the relatively high N content in the PEI-CCM indicated that the CCM was successfully modified by the PEI.

Table 1. Elemental Composition of the CCM and the Reused PEI-CCM

Element	CCM (wt%)	PEI-CCM (wt%)
C	92.5	81.0
O	7.51	12.1
N	—	6.85

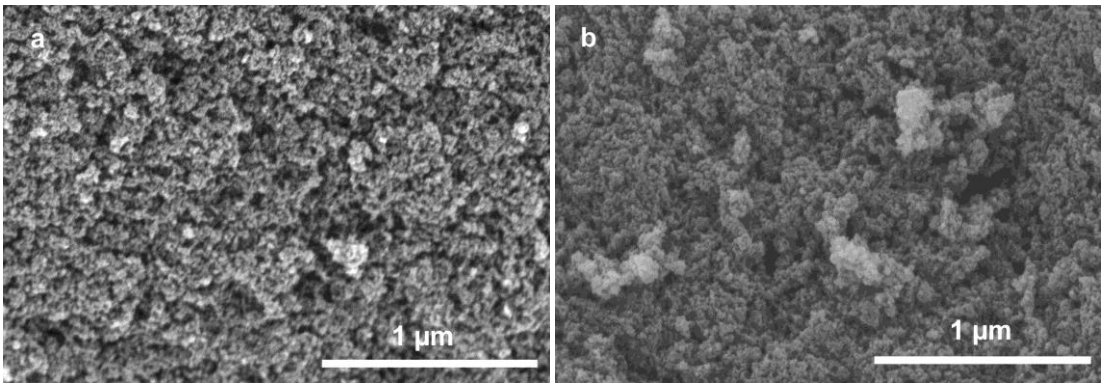

Fig. 1. FESEM surface images (a) CCM and (b) PEI-CCM

μmThe functional groups of the CCM, PEI, and PEI-CCM were analyzed by Fourier-transform infrared spectroscopy (FTIR), and the corresponding spectra are shown in Fig. 2. For the CCM, the band appearing beyond 3000 cm^{-1} resulted from the vibration of the O-H groups (Liu *et al*. 2019b). The bands appearing between 2800 cm^{-1} and 3000 cm^{-1} were attributed to the vibrations of the C-H groups (Hu *et al*. 2020). The band appearing at 1565 cm^{-1} was attributed to the vibration of C=O in carboxyl groups (Chen *et al*. 2018b). For the PEI, the bands appearing at 1585 cm^{-1} and 1450 cm^{-1} were attributed to the vibrations of N-H and C-N, respectively. For the PEI-CCM, compared with CCM, there was a new band appeared at 1450 cm^{-1} in the range from 1000 to 1500 cm^{-1}. Since the band at 1450 cm^{-1} comes from the vibration of C-N bond of PEI (Chen *et al*. 2018b), this result indicated that PEI was grafted on the surface of CCM. Compared with PEI, there was a new band of PEI-CCM appearing at 1635 cm^{-1}, which was assigned to the vibration of the amide groups (Geng *et al*. 2019). The presence of amide groups in the PEI-CCM suggests that the PEI was grafted onto the surface of the CCM through amide bond during the modification process.

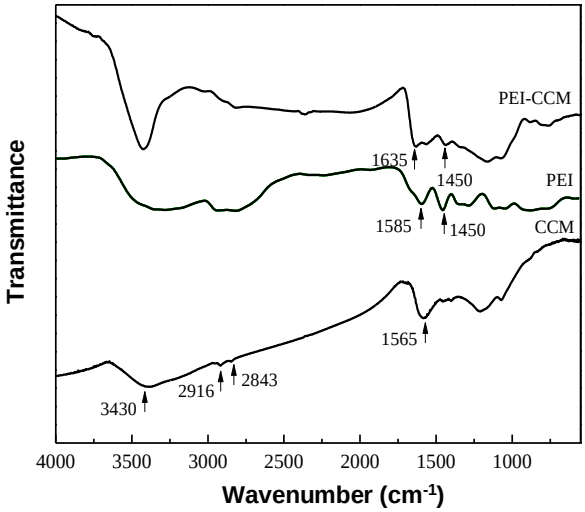

Fig. 2. FTIR spectra of CCM, PEI, and PEI-CCM

Pore structure can greatly affect the adsorption properties of an adsorbent (Liang *et al*. 2019). Thus, nitrogen adsorption-desorption isotherms of the CCM and PEI-CCM were determined, and the pore size distributions of the CCM and PEI-CCM were measured. The

results are presented in Fig. 3. The isotherm curves of the CCM and PEI-CCM were of type IV. Moreover, in the range of high relative pressure, the hysteresis loop was observed in both samples. The Brunauer-Emmett-Teller (BET) surface areas of the CCM and PEI-CCM were 1130 m^2/g and 519 m^2/g, respectively, while the pore diameters were 3.3 nm and 4.5 nm, respectively. Compared with the CCM, the BET surface area of the PEI-CCM decreased by 53.9%, while the pore diameter of the PEI-CCM increased by 36.4%. These observed changes were in accordance with the phenomenon of PEI blocking the micropores on the surface of porous material, leading to a decrease of the BET surface area and an increase of the pore diameter (Quan *et al*. 2019). The EDS, FTIR, and N_2 adsorption-desorption analyses all indicated that the CCM surface was successfully modified by the PEI.

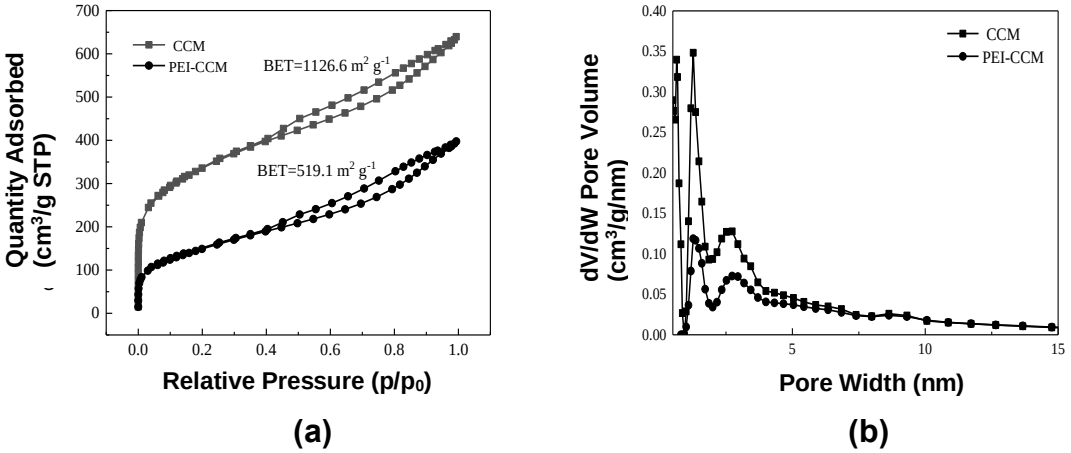

Fig. 3. (a) N_2 adsorption–desorption isotherms and (b) pore size distributions of CCM and PEI-CCM

Comparative Investigation on the Adsorption Abilities of PEI-CCM

When the CCM was modified by the PEI, which is a cationic polymer with many amine groups in its molecule, the surface properties of the CCM were greatly changed, leading to different adsorption abilities for the CCM and PEI-CCM. Figure 4 clarifies these differences, showing the adsorption capacities of the CCM and PEI-CCM in the adsorption of MO and Cr(VI). The CCM exhibited a high adsorption capacity for MO (392 mg/g) but a low adsorption capacity for Cr(VI) (12 mg/g). The PEI-CCM showed high adsorption capacity for both MO and Cr(VI) (316 mg/g and 123 mg/g, respectively). This phenomenon was due to the fact that, after CCM was modified by PEI, the electrostatic attraction between negatively charged chromate ions and the surface of adsorbent was strengthened (Hubbe *et al*. 2011; Geng *et al*. 2019). Meanwhile, the hydrogen bonding between the grafted PEI and MO made the adsorption of MO more easily for PEI-CCM (Li *et al*. 2018b). However, the greatly reduced BET surface area of PEI-CCM (Fig. 3a) decreased the MO adsorption capacity of PEI-CCM (Lv *et al*. 2018). Although the adsorption capacity for MO decreased by approximately 20% after the CCM was modified by the PEI, the Cr(VI) adsorption capacity of the PEI-CCM increased by more than nine times compared with the CCM, making the PEI-CCM a high-performance adsorbent for the adsorption of MO and Cr(VI).

Recently, the composition of pollutants in wastewater has become more and more complex. Developing the adsorbent with the ability to simultaneously remove heavy metal

ions and dyes has become an important research field. Many adsorbents which can simultaneously remove MO and Cr(VI) was developed. Table 2 presents the comparison of adsorption ability of various adsorbents for simultaneously removal of MO and Cr(VI) reported in literatures. It can be observed from Table 2 that, compared with NiFe-LDH and LDHs@PAB, MWCNTS@Fe_3O_4/PEI and PEI-CCM showed high MO adsorption performance with the adsorption capacity higher than 300 mg/g. Although MWCNTS@Fe_3O_4/PEI showed higher MO adsorption capacity, 596 mg/g, than PEI-CCM, 316 mg/g, the Cr(VI) adsorption capacity of MWCNTS@Fe_3O_4/PEI is lower than 50 mg/g, which is similar as that of NiFe-LDH and LDHs@PAB. Thus, PEI-CCM exhibited much better performance in the simultaneously removal of MO and Cr(VI). Moreover, the raw material of PEI-CCM came from the waste corncob. Using waste corncob to prepare the high-performance adsorbent, PEI-CCM, can be beneficial to the utilization of waste corncob and the environmental protection.

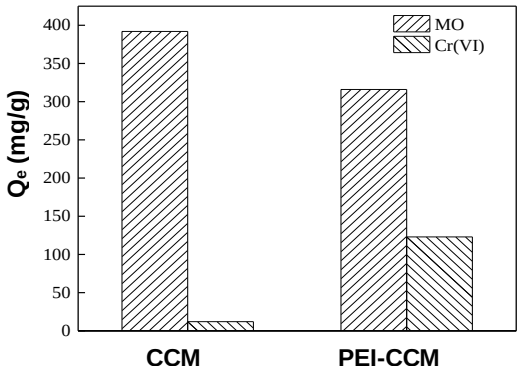

Fig. 4. MO adsorption capacities of CCM and PEI-CCM (temperature: 35 °C; initial concentrations: 100 mg/L; pH: 7.0; dosage: 0.2 g/L; adsorption time: 25 h) and Cr(VI) adsorption capacities of CCM and PEI-CCM (temperature: 35 °C; initial concentrations: 100 mg/L; pH: 5.7; dosage: 0.5 g/L; adsorption time: 1500 min)

Table 2. Comparison of Adsorption Capacities of Various Adsorbents for MO and Cr(VI)

Adsorbent	MO (Q_m (mg/g))	Cr(VI) (Q_m (mg/g))	References
NiFe-LDH	205	26	(Lu *et al*. 2016)
LDHs@PAB	186	49	(Chen *et al*. 2018a)
MWCNTS@Fe_3O_4/PEI	596	48	(Chen et al. 2019a)
PEI-CCM	316	123	This study

Adsorption Kinetics

The adsorption kinetics of the PEI-CCM for the removal of MO and Cr(VI) were determined, and the results are shown in Fig. 5. As the MO initial concentration increased, the MO adsorption capacity of the PEI-CCM also increased. When the MO initial concentration was increased from 50 mg/L to 200 mg/L, the MO adsorption capacity of the PEI-CCM increased from 250 mg/g to 374 mg/g. The Cr(VI) adsorption capacity of the PEI-CCM exhibited a similar tendency. When the Cr(VI) initial concentration was increased from 20 mg/L to 60 mg/L, the Cr(VI) adsorption capacity of the PEI-CCM increased from 40 mg/g to 83 mg/g. To investigate the adsorption mechanisms, the pseudo-first-order and pseudo-second-order kinetic models were applied to describe the adsorption

behavior of the adsorbent (Hubbe *et al*. 2012). Typically, the pseudo-first-order and pseudo-second-order kinetic models are expressed as in Eqs. 3 and 4,

$$\ln(Q_e - Q_t) = \ln Q_e - k_1 t \quad (3)$$

$$\frac{t}{Q_t} = \frac{1}{k_2 Q_e^2} + \frac{1}{Q_e} t \quad (4)$$

where Q_e (mg/g) is the adsorption capacity at adsorption equilibrium, Q_t (mg/g) is the adsorption capacity at time t (min), k_1 (1/min) is the rate constant of adsorption, and k_2 (g/(mg·min)) is the rate constant of the pseudo-second-order adsorption (Hou *et al*. 2013). The simulated results of the adsorption experimental data using these two kinetic models are presented in Tables 3 and 4. When the adsorption kinetic data for MO and Cr(VI) were simulated by the pseudo-second-order kinetic model, the corresponding correlation coefficient (R^2) was greater than that obtained with the pseudo-first-order kinetic model. This result demonstrates that the pseudo-second-order kinetic model was more suitable for describing the adsorption of MO and Cr(VI) by the PEI-CCM (Garba *et al*. 2020). Thus, the kinetic investigation results indicated that the adsorption rate of MO and Cr(VI) by the PEI-CCM is controlled by the time required procedure for the diffusion into narrow pores (Hubbe *et al*. 2019).

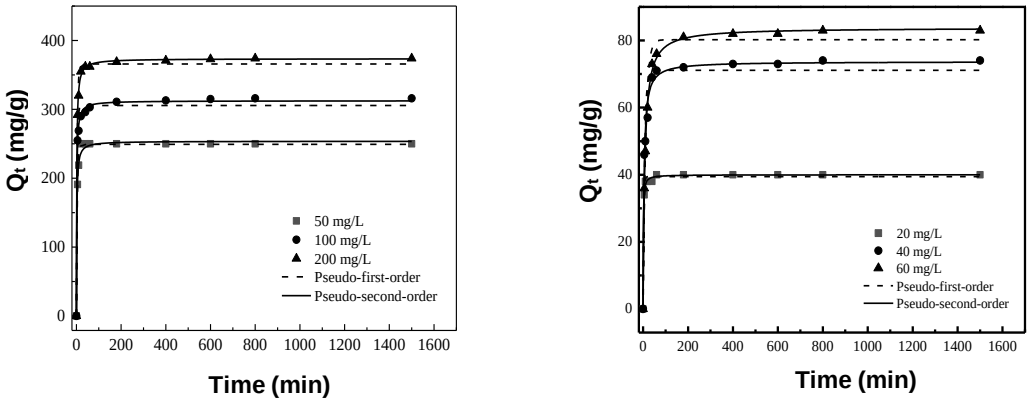

Fig. 5. (a) MO adsorption kinetic by the PEI-CCM at 35 °C (Conditions: initial concentrations: 50, 100, 200 mg/L; dosage: 0.2 g/L; pH: 7; adsorption time: 1500 min) and (b) Cr(VI) adsorption kinetic by the PEI-CCM at 35 °C (Conditions: initial concentrations: 20, 40, 60 mg/L; dosage: 0.5 g/L; pH: 5.7; adsorption time: 1500 min)

Table 3. MO Kinetic Adsorption Fitting Parameters

C_0	$Q_{e,exp}$	Pseudo-first-order			Pseudo-second-order		
		$Q_{e,cal}$	K_1	R^2	$Q_{e,cal}$	K_2	R^2
50	255	249.224	0.268	0.975	253.802	0.002	0.996
100	316	305.646	0.322	0.983	312.504	0.002	0.997
200	374	365.838	0.288	0.990	373.554	0.001	0.999

Table 4. Cr (VI) Kinetic Adsorption Fitting Parameters

C_0	$Q_{e,exp}$	Pseudo-first-order			Pseudo-second-order		
		$Q_{e,cal}$	K_1	R^2	$Q_{e,cal}$	K_2	R^2
20	40	39.445	0.388	0.985	40.001	0.030	0.997
40	74	71.096	0.146	0.952	73.708	0.003	0.988
60	83	80.202	0.086	0.977	83.789	0.001	0.997

Adsorption Isotherms

The Langmuir and Freundlich isotherm models are widely used to describe the adsorption behavior of adsorbents (Stawiński *et al*. 2017). Thus, these two models were used to describe the adsorption behavior of the PEI-CCM. The Langmuir and Freundlich isotherm models can be expressed by Eqs. 5 and 6,

$$\frac{1}{Q_e} = \frac{1}{Q_m K_L}\frac{1}{c_e} + \frac{1}{Q_m} \quad (5)$$

$$\log Q_e = \log K_F + \frac{1}{n}\log c_e \quad (6)$$

where Q_e (mg/g) is the adsorption capacity of the adsorbent for the adsorbate at adsorption equilibrium, Q_m (mg/g) is the maximum adsorption capacity of the adsorbent for the adsorbate, c_e (mg/L) is the concentration of adsorbate in solution at adsorption equilibrium, K_L (L/mg) is the Langmuir equilibrium constant, K_F ((mg/g) (L/mg) $^{1/n}$) is the Freundlich adsorption constant, and 1/*n* is the adsorption intensity (Yu *et al*. 2018).

The simulated adsorption curves for MO and Cr(VI) using the Langmuir and Freundlich isotherm models are shown in Fig. 6. Comparing the R^2 values, the adsorption experimental data for MO and Cr(VI) was better fitted by the Langmuir model compared to the Freundlich model. Because the Langmuir model is used to describe the behavior of monolayer adsorption, the isothermal adsorption results indicated that the adsorption of MO and Cr(VI) by the PEI-CCM was through the monolayer mode (Maneerung *et al*. 2016).

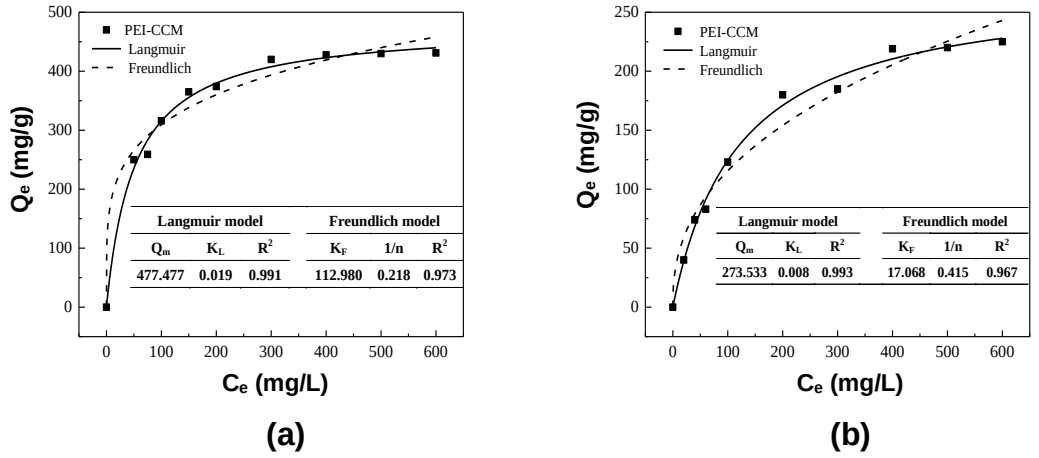

Fig. 6. (a) Isothermal adsorption of MO at 35 °C (Conditions: initial concentrations: 50 to 600 mg/L; dosage: 0.2 g/L; pH: 7) and (b) isothermal adsorption of Cr(VI) at 35 °C (Conditions: initial concentrations: 20 to 600 mg/L; dosage: 0.5 g/L; pH: 5.7)

Simultaneous Removal of MO and Cr(VI)

Figure 7 shows the differences between the CCM and PEI-CCM when they were applied for the simultaneous removal of MO and Cr(VI) in the simultaneous isothermal adsorption experiment. When the CCM was used for the simultaneous removal of MO and Cr(VI), the removal efficiency reached 100% for MO and 21% for Cr(VI). The PEI-CCM exhibited much better performance, with an MO removal efficiency of 100% and a Cr(VI)

removal efficiency of 95%. These results demonstrated that the PEI-CCM was a high-performance adsorbent for the simultaneous removal of MO and Cr(VI).

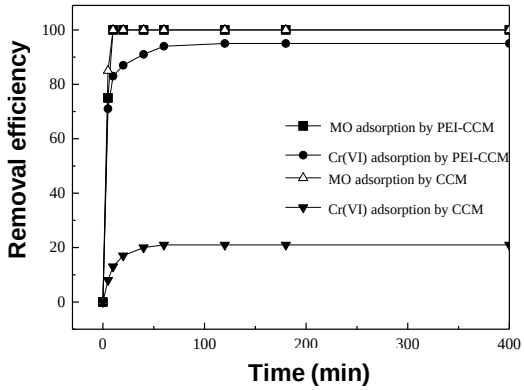

Fig. 7. Comparison of the simultaneous removal of MO and Cr(VI) by the CCM and PEI-CCM (temperature: 35 °C; initial concentrations: 20 mg/L; pH: 5.7; dosage: 0.5 g/L; adsorption time: 400 min)

Reusability of the PEI-CCM Adsorbent

Reusability is an important characteristic for an adsorbent. Although the PEI-CCM exhibited a high adsorption capacity, its reusability still needed to be examined. As shown in Fig. 8, the regenerated PEI-CCM showed high reusability for the removal of MO and Cr(VI). The MO removal efficiency decreased by less than 3% after being reused four times. Meanwhile, the Cr(VI) removal efficiency decreased by approximately 16% after four times of reuse, which is still acceptable for the purification of industrial-scale polluted water (Chen *et al*. 2019b; Tangtubtim and Saikrasun 2019). The good reusability of the PEI-CCM adsorbent supports its potential industrial application for the treatment of polluted water containing both heavy metal and dye pollutants.

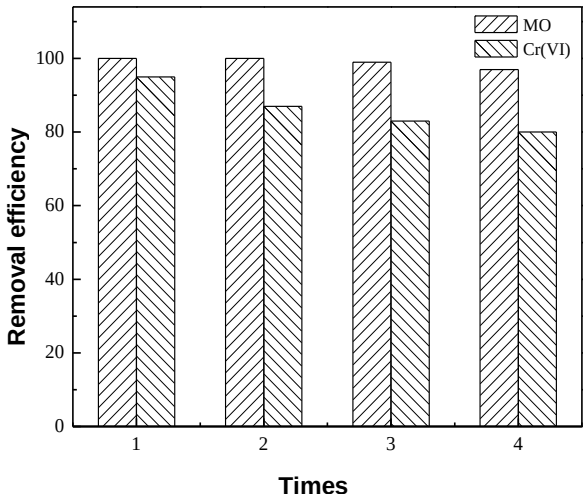

Fig. 8. Reusability of the PEI-CCM adsorbent (Conditions: Temperature: 35 °C; initial concentrations: 20 mg/L; pH: 5.7; dosage: 0.5 g/L; adsorption time: 400 min).

CONCLUSIONS

1. Polyethyleneimine-modified corncob-derived carbon material (PEI-CCM) was prepared and successfully applied for the adsorption of methyl orange dye (MO) and Cr(VI). The structural characterization of the PEI-CCM indicated that the PEI was grafted onto the CCM surface through amide bonds. The adsorption behavior of the PEI-CCM for MO and Cr(VI) was in accordance with the pseudo-second-order kinetic model and the Langmuir isotherm model.
2. In the experiment of simultaneous adsorption of MO and Cr(VI), the PEI-CCM exhibited high removal efficiencies: 100% for MO and 95% for Cr(VI). Moreover, the PEI-CCM showed excellent recycling performance, supporting its use as a low-cost and high-performance adsorbent for the treatment of complexly polluted water.

ACKNOWLEDGMENTS

This work was funded by the Open Research Fund of the State Key Laboratory of Polymer Physics and Chemistry, Changchun Institute of Applied Chemistry, Chinese Academy of Sciences (No. 2018-02); the Key Laboratory for Catalyst Synthesis Technology of Polymer of Liaoning Province, China (No. 2010-36); and the General Project Fund of Liaoning Education Department (No. LJGD2019014).

REFERENCES CITED

Amin, M. T., Alazba, A. A., and Shafiq, M. (2019). "Comparative study for adsorption of methylene blue dye on biochar derived from orange peel and banana biomass in aqueous solutions," *Environmental Monitoring and Assessment* 191(12). DOI: 10.1007/s10661-019-7915-0

Chen, B., Chen, S., Zhao, H., Liu, Y., Long, F., and Pan, X. (2019a). "A versatile β-cyclodextrin and polyethyleneimine bi-functionalized magnetic nanoadsorbent for simultaneous capture of methyl orange and Pb(II) from complex wastewater," *Chemosphere* 216, 605-616. DOI: 10.1016/j.chemosphere.2018.10.157

Chen, B., Yue, W., Zhao, H., Long, F., Cao, Y., and Pan, X. (2019b). "Simultaneous capture of methyl orange and chromium(VI) from complex wastewater using polyethylenimine cation decorated magnetic carbon nanotubes as a recyclable adsorbent," *RSC Advances* 9(9), 4722-4734. DOI: 10.1039/c8ra08760a

Chen, R., Zhai, S., Lu, W., Wei, J., Xu, J., Lu, A., and Jiang, H. (2020). "Facile one-pot solvothermal synthesis of magnetic mesoporous carbon for the efficient adsorption of methyl orange," *Environmental Science and Pollution Research* 27(8), 8248-8259. DOI: 10.1007/s11356-019-07492-x

Chen, S., Huang, Y., Han, X., Wu, Z., Lai, C., Wang, J., Deng, Q., Zeng, Z., and Deng, S. (2018a). "Simultaneous and efficient removal of Cr(VI) and methyl orange on LDHs decorated porous carbons," *Chemical Engineering Journal* 352, 306-315. DOI: 10.1016/j.cej.2018.07.012

Chen, S., Wang, J., Wu, Z., Deng, Q., Tu, W., Dai, G., Zeng, Z., and Deng, S. (2018b). "Enhanced Cr(VI) removal by polyethylenimine- and phosphorus-codoped

hierarchical porous carbons," *Journal of Colloid and Interface Science* 523, 110-120. DOI: 10.1016/j.jcis.2018.03.057

de Freitas, F., Battirola, L. D., Arruda, R., and de Andrade, R. L. T. (2019). "Assessment of the Cu(II) and Pb(II) removal efficiency of aqueous solutions by the dry biomass Aguapé: Kinetics of adsorption," *Environmental Monitoring and Assessment* 191(12). DOI: 10.1007/s10661-019-7933-y

Gao, H., Song, Z., Zhang, W., Yang, X., Wang, X., and Wang, D. (2017). "Synthesis of highly effective absorbents with waste quenching blast furnace slag to remove methyl orange from aqueous solution," *Journal of Environmental Sciences* 53, 68-77. DOI: 10.1016/j.jes.2016.05.014

Garba, Z. N., Lawan, I., Zhou, W., Zhang, M., Wang, L., and Yuan, Z. (2020). "Microcrystalline cellulose (MCC) based materials as emerging adsorbents for the removal of dyes and heavy metals – A review," *Science of the Total Environment* 717. DOI: 10.1016/j.scitotenv.2019.135070

Geng, J., Yin, Y., Liang, Q., Zhu, Z., and Luo, H. (2019). "Polyethyleneimine cross-linked graphene oxide for removing hazardous hexavalent chromium: Adsorption performance and mechanism," *Chemical Engineering Journal* 361, 1497-1510. DOI: 10.1016/j.cej.2018.10.141

Hou, X.-X., Deng, Q.-F., Ren, T.-Z., and Yuan, Z.-Y. (2013). "Adsorption of Cu^{2+} and methyl orange from aqueous solutions by activated carbons of corncob-derived char wastes," *Environmental Science and Pollution Research* 20(12), 8521-8534. DOI: 10.1007/s11356-013-1792-9

Hu, L., Guang, C., Liu, Y., Su, Z., Gong, S., Yao, Y., and Wang, Y. (2020). "Adsorption behavior of dyes from an aqueous solution onto composite magnetic lignin adsorbent," *Chemosphere* 246. DOI: 10.1016/j.chemosphere.2019.125757

Hubbe, M. A., Azizian, S., and Douven, S. (2019). "Implications of apparent pseudo-second-order adsorption kinetics onto cellulosic materials: A review," *BioResources* 14(3), 7582-7626.

Hubbe, M. A., Beck, K. R., O'Neal, W. G., and Sharma, Y. C. (2012). "Cellulosic substrates for removal of pollutants from aqueous systems: A review. 2 . Dyes," *BioResources* 7(2), 2592-2687.

Hubbe, M. A., Hasan, S. H., and Ducoste, J. J. (2011). "Cellulosic substrates for removal of pollutants from aqueous systems: A review. 1. Metals," *BioResources* 6(2), 2161-2287. DOI: 10.15376/biores.6.2.2161-2287

Laleicke, P. F. (2018). "Wood waste, the challenges of communication and innovation," *BioResources* 13(2), 2182-2183. DOI: 10.15376/biores.13.2.2182-2183

Li, H., Gao, P., Cui, J., Zhang, F., Wang, F., and Cheng, J. (2018a). "Preparation and Cr(VI) removal performance of corncob activated carbon," *Environmental Science and Pollution Research* 25(21), 20743-20755. DOI: 10.1007/s11356-018-2026-y

Li, J., Michalkiewicz, B., Min, J., Ma, C., Chen, X., Gong, J., Mijowska, E., and Tang, T. (2019). "Selective preparation of biomass-derived porous carbon with controllable pore sizes toward highly efficient CO_2 capture," *Chemical Engineering Journal* 360, 250-259. DOI: 10.1016/j.cej.2018.11.204

Li, X., Wang, Z., Ning, J., Gao, M., Jiang, W., Zhou, Z., and Li, G. (2018b). "Preparation and characterization of a novel polyethyleneimine cation-modified persimmon tannin bioadsorbent for anionic dye adsorption," *Journal of Environmental Management* 217, 305-314. DOI: 10.1016/j.jenvman.2018.03.107

Liang, H., Song, B., Peng, P., Jiao, G., Yan, X., and She, D. (2019). "Preparation of

three-dimensional honeycomb carbon materials and their adsorption of Cr(VI)," *Chemical Engineering Journal* 367, 9-16. DOI: 10.1016/j.cej.2019.02.121

Liu, H., Wang, Z., Li, H., Wang, H., and Yu, R. (2018). "Controlled synthesis of silkworm cocoon-like α-Fe_2O_3 and its adsorptive properties for organic dyes and Cr(VI)," *Materials Research Bulletin* 100, 302-307. DOI: 10.1016/j.materresbull.2017.12.030

Liu, X., Ma, C., Li, J., Zielinska, B., Kalenczuk, R. J., Chen, X., Chu, P. K., Tang, T., and Mijowska, E. (2019a). "Biomass-derived robust three-dimensional porous carbon for high volumetric performance supercapacitors," *Journal of Power Sources* 412, 1-9. DOI: 10.1016/j.jpowsour.2018.11.032

Liu, Y.-L., Li, Y.-T., Huang, J.-F., Zhang, Y.-L., Ruan, Z.-H., Hu, T., Wang, J.-J., Li, W.-Y., Hu, H.-J., and Jiang, G.-B. (2019b). "An advanced sol–gel strategy for enhancing interfacial reactivity of iron oxide nanoparticles on rosin biochar substrate to remove Cr(VI)," *Science of the Total Environment* 690, 438-446. DOI: 10.1016/j.scitotenv.2019.07.021

Lu, Y., Jiang, B., Fang, L., Ling, F., Gao, J., Wu, F., and Zhang, X. (2016). "High performance NiFe layered double hydroxide for methyl orange dye and Cr(VI) adsorption," *Chemosphere* 152, 415-422. DOI: 10.1016/j.chemosphere.2016.03.015

Lv, Z., Yang, S., Liu, Y., Zhou, J., Xing, L., and Chen, L. (2018). "The novel PEI-modified biochars and their application for the efficient elimination of Cr(VI) from aqueous solutions," *Water Science and Technology* 77(8), 2045-2056. DOI: 10.2166/wst.2018.118

Ma, Y., Liu, W.-J., Zhang, N., Li, Y.-S., Jiang, H., and Sheng, G.-P. (2014). "Polyethylenimine modified biochar adsorbent for hexavalent chromium removal from the aqueous solution," *Bioresource Technology* 169, 403-408. DOI: 10.1016/j.biortech.2014.07.014

Maneerung, T., Liew, J., Dai, Y., Kawi, S., Chong, C., and Wang, C.-H. (2016). "Activated carbon derived from carbon residue from biomass gasification and its application for dye adsorption: Kinetics, isotherms and thermodynamic studies," *Bioresource Technology* 200, 350-359. DOI: 10.1016/j.biortech.2015.10.047

Mishra, S., and Maiti, A. (2019). "Study of simultaneous bioremediation of mixed reactive dyes and Cr(VI) containing wastewater through designed experiments," *Environmental Monitoring and Assessment* 191(12). DOI:10.1007/s10661-019-7976-0

Norouzi, S., Heidari, M., Alipour, V., Rahmanian, O., Fazlzadeh, M., Mohammadi-moghadam, F., Nourmoradi, H., Goudarzi, B., and Dindarloo, K. (2018). "Preparation, characterization and Cr(VI) adsorption evaluation of NaOH-activated carbon produced from date press cake; an agro-industrial waste," *Bioresource Technology* 258, 48-56. DOI: 10.1016/j.biortech.2018.02.106

Pan, Y., and Zhao, H. (2019). "A green method to fabricate polyethyleneimine-alginate multilayer coatings modified polyurethane foam for Cu^{2+} adsorption from aqueous solution," *Polymer-Plastics Technology and Materials* 58(4), 384-393. DOI: 10.1080/03602559.2018.1471715

Quan, X., Sun, Z., Meng, H., Han, Y., Wu, J., Xu, J., Xu, Y., and Zhang, X. (2019). "Polyethyleneimine (PEI) incorporated Cu-BTC composites: Extended applications in ultra-high efficient removal of congo red," *Journal of Solid State Chemistry* 270, 231-241. DOI: 10.1016/j.jssc.2018.11.021

Rahim, A. R. A., Rabat, N. E., Johari, K., Saman, N., and Mat, H. (2019). "Removal of lead (II) ions from aqueous solution using desiccated coconut waste as low-cost

adsorbent," *Chemical Engineering Transactions* 72, 169-174. DOI: 10.3303/CET1972029

Rathinam, K., Singh, S. P., Arnusch, C. J., and Kasher, R. (2018). "An environmentally-friendly chitosan-lysozyme biocomposite for the effective removal of dyes and heavy metals from aqueous solutions," *Carbohydrate Polymers* 199, 506-515. DOI: 10.1016/j.carbpol.2018.07.055

Santos, C. M., Dweck, J., Viotto, R. S., Rosa, A. H., and de Morais, L. C. (2015). "Application of orange peel waste in the production of solid biofuels and biosorbents," *Bioresource Technology* 196, 469-479. DOI: 10.1016/j.biortech.2015.07.114

Singh, S. P., Rathinam, K., Kasher, R., and Arnusch, C. J. (2018). "Hexavalent chromium ion and methyl orange dye uptake *via* a silk protein sericin-chitosan conjugate," *RSC Advances* 8(48), 27027-27036. DOI: 10.1039/c8ra03907k

Stawiński, W., Węgrzyn, A., Freitas, O., Chmielarz, L., Mordarski, G., and Figueiredo, S. (2017). "Simultaneous removal of dyes and metal cations using an acid, acid-base and base modified vermiculite as a sustainable and recyclable adsorbent," *Science of the Total Environment* 576, 398-408. DOI: 10.1016/j.scitotenv.2016.10.120

Song, X. Y., Pan, G. X., Bai, Y. W., Liang, F., Xing, J. J., Gao, J., and Shi, F. N. (2019). "Preparation and electrochemical properties of biochar from pyrolysis of pomelo peel via different methods," *Fullerenes Nanotubes and Carbon Nanostructures* 7(5), 453-458. DOI: 10.1080/1536383X.2019.1597858

Sun, Y., Li, H., Li, G., Gao, B., Yue, Q., and Li, X. (2016). "Characterization and ciprofloxacin adsorption properties of activated carbons prepared from biomass wastes by H_3PO_4 activation," *Bioresource Technology* 217, 239-244. DOI: 10.1016/j.biortech.2016.03.047

Tangtubtim, S., and Saikrasun, S. (2019). "Adsorption behavior of polyethyleneimine-carbamate linked pineapple leaf fiber for Cr(VI) removal," *Applied Surface Science* 467-468, 596-607. DOI: 10.1016/j.apsusc.2018.10.204

Wang, S., Wang, J., Sun, P., Xu, L., Okoye, P. U., Li, S., Zhang, L., Guo, A., Zhang, J., and Zhang, A. (2019). "Disposable baby diapers waste derived catalyst for synthesizing glycerol carbonate by the transesterification of glycerol with dimethyl carbonate," *Journal of Cleaner Production* 211, 330-341. DOI: 10.1016/j.jclepro.2018.11.196

Wang, S., Wang, J., Okoye, P. U., Chen, S., Li, X., Duan, L., Zhou, H., Li, S., Tao, T., Zhang, L., *et al*. (2020a). "Application of corncob residue-derived catalyst in the transesterification of glycerol with dimethyl carbonate to synthesize glycerol carbonate," *BioResources* 15(1), 142-158. DOI: 10.15376/biores.15.1.142-158

Wang, W., Hu, B., Wang, C., Liang, Z., Cui, F., Zhao, Z., and Yang, C. (2020b). "Cr(VI) removal by micron-scale iron-carbon composite induced by ball milling: The role of activated carbon," *Chemical Engineering Journal* 389. DOI: 10.1016/j.cej.2019.122633

Wen, X., Liu, H., Zhang, L., Zhang, J., Fu, C., Shi, X., Chen, X., Mijowska, E., Chen, M.-J., and Wang, D.-Y. (2019). "Large-scale converting waste coffee grounds into functional carbon materials as high-efficient adsorbent for organic dyes," *Bioresource Technology* 272, 92-98. DOI: 10.1016/j.biortech.2018.10.011

Yu, J., Jiang, C., Guan, Q., Ning, P., Gu, J., Chen, Q., Zhang, J., and Miao, R. (2018). "Enhanced removal of Cr(VI) from aqueous solution by supported ZnO nanoparticles on biochar derived from waste water hyacinth," *Chemosphere* 195, 632-640. DOI:

10.1016/j.chemosphere.2017.12.128
Zhang, S., Shi, X., Wróbel, R., Chen, X., and Mijowska, E. (2019). "Low-cost nitrogen-doped activated carbon prepared by polyethylenimine (PEI) with a convenient method for supercapacitor application," *Electrochimica Acta* 294, 183-191. DOI: 10.1016/j.electacta.2018.10.111
Zhang, Y., Jiao, X., Liu, N., Lv, J., and Yang, Y. (2020). "Enhanced removal of aqueous Cr(VI) by a green synthesized nanoscale zero-valent iron supported on oak wood biochar," *Chemosphere* 245. DOI: 10.1016/j.chemosphere.2019.125542
Zheng, Y., Cheng, B., You, W., Yu, J., and Ho, W. (2019). "3D hierarchical graphene oxide-NiFe LDH composite with enhanced adsorption affinity to Congo red, methyl orange and Cr(VI) ions," *Journal of Hazardous Materials* 369, 214-225. DOI: 10.1016/j.jhazmat.2019.02.013

Article submitted: June 9, 2020; Peer review completed: July 25, 2020; Revised version received: July 29, 2020; Accepted: July 30, 2020; Published: August 5, 2020.
DOI: 10.15376/biores.15.4.7342-7356